REVIEW OF e^+e^- REACTIONS IN THE ENERGY RANGE 3 TO 9 GeV *

Jasper Kirkby
Stanford Linear Accelerator Center
Stanford University, Stanford, California 94305

SLAC-PUB-2419
October 1979
(T/E)

Summary

The current experimental status of the τ and charmed particles in medium-energy e^+e^- annihilations is reviewed.

I. Introduction

There are three principal subjects explored by e^+e^- annihilations in the DORIS I/SPEAR energy range: jets, the τ lepton and charm. The subtle indication of jets at these low energies can now be contrasted with the visually-striking PETRA data, which has provided new insights into the jet characteristics Accordingly, my discussion will be limited to the τ and charm. As we shall see, our relative understanding of these subjects has essentially reversed since the VIII Lepton Photon Symposium at Hamburg. The general properties of the τ and most of its decay modes have now been measured fairly precisely and found to agree with the "standard model", whereas the charmed particles have recently provided some unexpected results.

I will attempt to bring out the salient information provided by the experiments at DORIS and SPEAR. In the short time available for this talk it is impossible to give credit to all the measurements of each quantity and so, where appropriate, I will simply present the data with the highest statistics. The topics which will be discussed in the following sections are:

II. The τ lepton
III. The hadronic cross-section and charmonium
IV. The F mesons
V. The charmed baryons
VI. The D mesons
VII. The charm lifetime

II. The τ Lepton

A. General Properties

At the time of the 1977 Hamburg Conference there were still reservations that the τ might be an obscure manifestation of charm — a feeling motivated in part by the close proximity of the threshold for the two processes. The final doubts were eliminated later that year by the DASP group[1] which observed τ decays at the ψ', manifestly below charm threshold. They determined the τ mass to be (1807 ± 20) MeV/c^2 and, shortly thereafter, values were quoted from DELCO[1] of (1782^{+3}_{-4}) MeV/c^2 and DESY-HEIDELBERG[1] of (1787^{+10}_{-18}) MeV/c^2. The DELCO measurement followed from a detailed mapping (Fig. 1) of the production cross-section of events containing one electron and one non-electron. These so-called "anomalous two-prong electron events" are found to contain almost exclusively the decay products of a $\tau^+\tau^-$ pair. The abrupt rise in cross-section at threshold excludes integer spin assignments for the τ since this would require p-wave production ($\propto\beta_\tau^3$) in order to conserve parity. However, half-integer spin particles can be produced in an s-wave which results in a threshold cross-section $\propto\beta_\tau$, compatible with observation. The distinction between different half-integer spins occurs at higher energies where the cross-section for spins greater than ½ becomes divergent[2] (Fig. 2) on the assumption of the absence of anomalous form factors. Independent confirmation of the spin ½ assignment is obtained from the $\tau^- \to \pi^-\nu_\tau$ branching ratio as discussed below.[3]

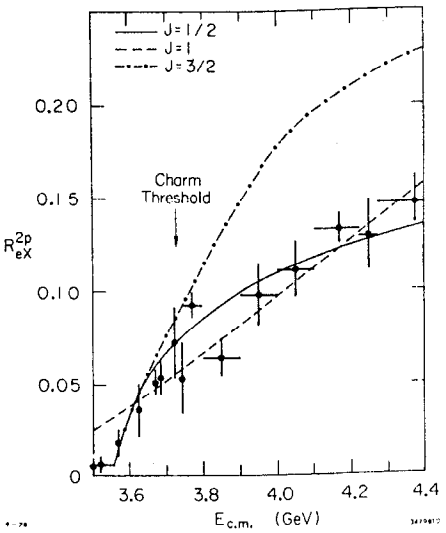

Fig. 1. The two-prong electron cross-section ratio, $R_{eX} = \sigma(eX)/\sigma_{\mu\mu}$ measured by DELCO in the center-of-mass energy range, $3.50 < E_{cm} < 4.4$ GeV. The fitted curves indicate the threshold behavior for a pair of particles with spin ½ (solid), 1 (dashed) and 3/2 (dot-dashed).

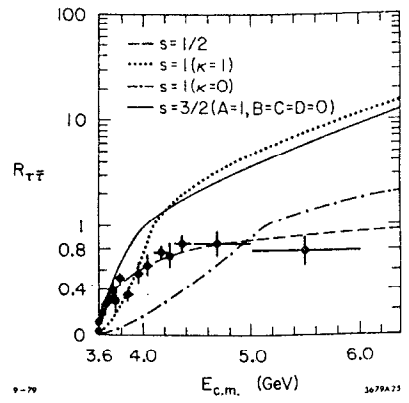

Fig. 2. The cross-sections expected for a pair of point-like particles according to several spin assignments. The constants κ, A, B, C and D are related to the gyromagnetic ratio and multipole values of the particles (see Ref. 2 for details). The data points are the DELCO eX events, normalized to the spin ½ curve. Note that the vertical scale changes from linear to logarithmic at 1.0.

In summary, the cross-section indicates a new threshold for a pair of spin ½ particles and displays a smooth rise to a constant value, relative to $\mu^+\mu^-$ production, as betokens point-like particles. These characteristics exclude a hadron description but are precisely those of a "heavy" lepton.

Under the assumption that the standard weak current participates in τ decays, the lifetime in $\tau_0 = \tau_\mu \times (m_\mu/m_\tau)^5 b_e$, where τ_μ = μ lifetime, m_l = lepton mass and b_e = branching ratio for $\tau^- \to \nu_\tau e^-\bar{\nu}_e$. Experimentally, $b_e = (0.175 \pm 0.011)$ and so $\tau_0 = (2.8 \pm 0.2)\ 10^{-13}$ sec. At these energies, the lifetime allows a τ flight-path of about 0.2 mm, approximately a factor of 4 less than the average transverse dimension of the SPEAR interaction volume. Although this flight-path is not measurable without far larger data samples, an upper limit of approximately 1 mm has been placed by DELCO.[4] The technique is to use the observed three-momenta in the two-prong

* Work supported in part by the National Science Foundation, and in part by the Department of Energy under contract number DE-AC03-76SF00515.

(Invited talk at the IX International Symposium on Lepton & Photon Integrations at High Energies, Batavia, Illinois, August 23-29, 1979.)

eX events in order to reconstruct weighted probability distributions of the initial τ directions and in turn to compute weighted flight-path measurements. The final result is the τ lifetime limit, $\tau_0 < 2.3\ 10^{-12}$ sec (95% CL). This is equivalent to a lower limit on the coupling strength at the $\tau - \nu_\tau - W$ vertex of 12% (95% CL) of full weak strength. It is interesting to note that at the highest PETRA/PEP energies the τ flight-path is 0.8 mm and so a finite measurement of the lifetime may be possible.

The V,A structure of the $\tau - \nu_\tau$ vertex has been measured from the electron energy spectrum in the decay $\tau^- \to \nu_\tau e^- \bar{\nu}_e$. (Throughout, this notation implies both charge-conjugate reactions, unless otherwise indicated.) The predicted spectrum is shown in Fig. 3 under the

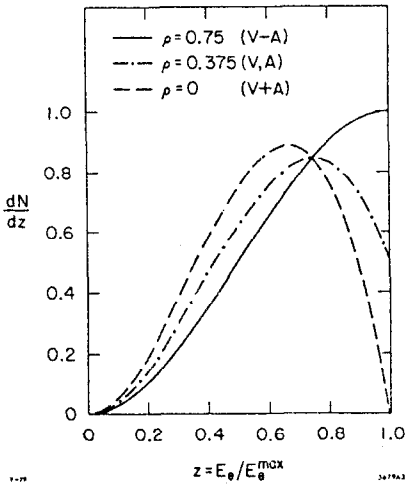

Fig. 3. The (non-radiatively-corrected) normalized electron energy spectrum in the τ rest-frame for the decay $\tau^- \to \nu_\tau e^- \bar{\nu}_e$ under several space-time assumptions for the $\tau - \nu_\tau$ coupling.

assumption that $e - \nu_e$ vertex is pure V - A. The most general coupling is a linear combination of V and A amplitudes but, for a massless ν_τ, the anticipated couplings are pure V - A or V + A which correspond, respectively, to a left-handed ν_τ and a right-handed ν_τ. These spectra are characterized by the Michel parameter, ρ, which is 0.75 for V - A and 0 for V + A.

The experimental data[4] (Fig. 4) is well fitted by a V - A spectrum, whereas V + A is completely excluded and pure V or pure A are disfavored. If the Michel parameter is left free before fitting this data, it is found to have the value $\rho = 0.72 \pm 0.15$ (χ^2/dof = 15.8/16), after including systematic errors. A separation between the V - A and the V + A hypotheses has been suggested by Nachtmann and Pais[5] for experimental data with limited statistics. They point out that the mean value of the electron energy divided by the beam energy should be 0.35 and 0.30 for V - A and V + A, respectively, under the conditions of complete acceptance, no measurement errors and no radiative corrections. The application of this test in the DELCO data[4] (Fig. 5) indicates there is agreement with V - A throughout the full center-of-mass energy range.

The electron energy spectrum is also sensitive to the mass of the ν_τ. Since the V + A hypothesis is ruled out for any value of the ν_τ mass, the measurement is made by assuming V - A and determining the χ^2 of the fitted curves versus ν_τ mass. In this fashion, the data of Fig. 4 provides the τ neutrino mass upper limit of 250 MeV/c^2 (95% CL).

All these properties can be combined into the Feynman graph of the decay $\tau^- \to \nu_\tau e^- \bar{\nu}_e$ (Fig. 6).

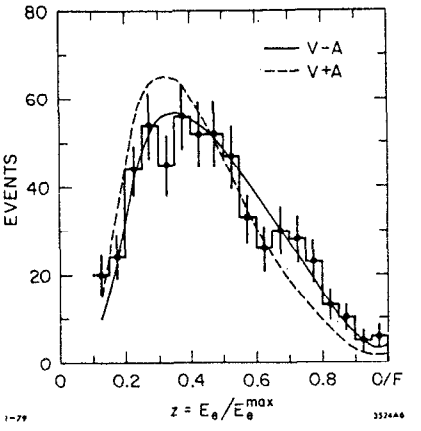

Fig. 4. The normalized electron energy spectrum obtained by DELCO in the energy range, $3.57 < E_{cm} < 7.5$ GeV (excluding ψ"). The radiatively-corrected fits for V - A (solid) and V + A (dashed) show χ^2/dof of 15.9/17 and 53.7/17, respectively.

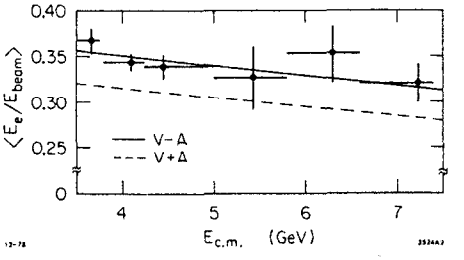

Fig. 5. The electron energy divided by the beam energy for the data of Fig. 4, separated into several center-of-mass energy ranges. The predictions of the V - A and V + A hypotheses are indicated by the solid and dashed lines, respectively, after accounting for radiative corrections, losses and measurement errors.

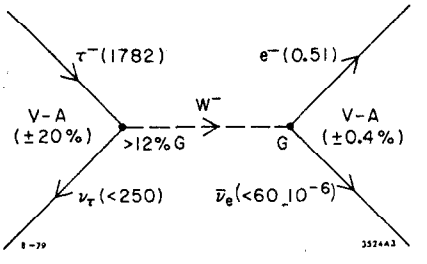

Fig. 6. A diagram of the decay $\tau^- \to \nu_\tau e^- \bar{\nu}_e$ which compares the experimental knowledge of $\tau - \nu_\tau$ with that of $e - \nu_e$. The particle-masses are given in the units MeV/c^2

The close analogy between $\tau - \nu_\tau$ (left-hand side) and $e - \nu_e$ (right-hand side) is striking.

B. Branching Ratios

The majority of the τ decay rates can be calculated and so branching-ratio measurements provide further tests of whether the standard weak current participates in τ decays.

The world average branching ratios and theoretical predictions are summarized in Table I. The experimental measurements made before November, 1978 are referenced by Feldman.[6] Only the new data, available since that time, will be discussed here. The theoretical predictions have been derived from recent rate calculations[7] after normalizing the total contribution, including Cabibbo suppressed modes, to 100%. However, where experiments have excluded the kaon contributions, Table I shows the comparable theoretical calculation in parentheses.

All the new information on τ one-prong decays has been provided by Dorfan and co-workers using data taken by the Mark II detector[8] at SPEAR. They have measured the branching ratio to $\pi^-X^+ + 0\gamma$, observed in the energy range, $4.5 < E_{cm} < 6.0$ GeV. The major background, which constitutes 35% of the observed events, is provided by the decay $\tau^- \to \rho^-\nu_\tau$ in which both photons excape detection. After removal of the backgrounds, the π energy distribution (Fig. 7) displays the box-like shape which is characteristic of a two-body decay. The measured branching ratio is $b(\tau^- \to \pi^-\nu_\tau) = (10.7 \pm 2.0)\%$.

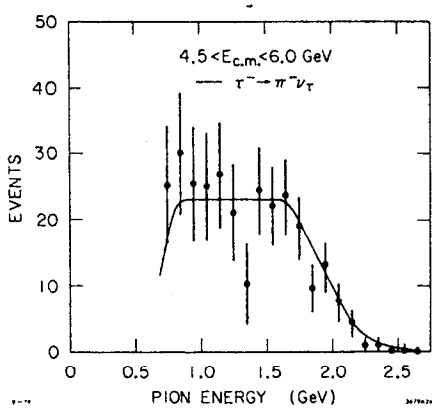

Fig. 7. The π energy spectrum observed by the Mark II for the decay $\tau^- \to \pi^-\nu_\tau$ in the energy range, $4.5 < E_{cm} < 6.0$ GeV.

The $\pi^-\nu_\tau$ decay mode has now been observed by four experiments which collectively measure a branching ratio in agreement with theoretical expectations. The $\pi^-\nu_\tau$ branching ratio measurement provides additional information which supports the spin ½ assignment for the τ and the ν_τ. A comparison of the theoretical calculations[9] with the experimental measurement of $\Gamma(\tau^- \to \pi^-\nu_\tau)/\Gamma(\tau^- \to e^-\bar{\nu}_e\nu_\tau)$ {Table II} excludes a spin 3/2 assignment for the τ or ν_τ. The relative rates vary since different τ and ν_τ spins alter the mass, and thereby the branching ratios, of the virtual W in the decay $\tau^- \to \nu_\tau W^-$. In the case of a (τ,ν_τ) spin of (½,3/2), helicity-conservation forbids the $\pi^-\nu_\tau$ mode. The effects of spin values ≥ 5/2 have not been calculated.

Table II. A Comparison of the Predicted and Observed πν Decay Rate for Several (τ,ν_τ) Spin Assignments

(τ,ν_τ) SPIN	(½,½)	(½,3/2)	(3/2,½)	(3/2,3/2)
$\{\Gamma(\pi\nu)/\Gamma(e\nu\nu)\}_{THEORY}$	0.59	0	0.25	1.33
$\{\Gamma(\pi\nu)/\Gamma(e\nu\nu)\}_{EXPERIMENT}$ = 0.52 ± 0.07				

The Mark II detector has also provided new information on the decay $\tau^- \to \pi^-\pi^0\nu_\tau$ based on a sample of 93 events of the type $\pi^-\pi^0 l^+$, $l = e,\mu$. The lepton requirement serves both to decrease the non-τ background and to remove any ambiguity in the $\pi^-\pi^0$ invariant mass measurement. The latter quantity is plotted in Fig. 8 and clearly indicates the dominance of ρ production

Table I. World-Average τ Branching Ratios and Theoretical Predictions

Final State	Branching Ratio (%) Experimental	Theoretical*
a) 1-Prong:		
$\nu_\tau e^-\bar{\nu}_e$	17.5 ± 1.1	18.0
$\nu_\tau \mu^-\bar{\nu}_\mu$	18.5 ± 1.2	17.5
$\nu_\tau \pi^-$	9.1 ± 1.1	11.1 (10.6)
$\nu_\tau \rho^-$	20.9 ± 3.7	23.4 (22.4)
	66.0 ± 4.2	70.0
$\nu_\tau \pi^- \geq 2\pi^0$	---	10.0
b) Multi-Prong		
$\nu_\tau \pi^-\pi^-\pi^+$	5.6 ± 1.6	4.3
$\nu_\tau \pi^-\pi^-\pi^+ \geq 1\pi^0$	---	14.4
$\nu_\tau 3\pi^- 2\pi^+ \geq 0\pi^0$	---	1.3
$\nu_\tau \geq$ 3-charged-particles $\geq 0\pi^0$	28. ± 6.	20.0
Observed Total	94. ± 7.	90.0
c) Exotica		
3X (X = charged particle)	< 1.0 (95% CL)	0
3l (l = lepton)	< 0.6 (90% CL)	0
1 + nX	< 4.0 (90% CL)	0
1 + nγ	< 12.0 (90% CL)	0
$e^-\gamma$	< 2.6 (90% CL)	0
$\mu^-\gamma$	< 1.3 (90% CL)	0

*Unless shown in parentheses, the theoretical branching ratios include the contributions from K's to the hadronic final states.

(a Breit-Wigner resonance fit finds $M_\rho = 770 \pm 20$ MeV/c^2 and $\Gamma_\rho = 194 \pm 30$ MeV/c). This is exactly what was anticipated from e^+e^- measurements at $\sqrt{s} < m_\tau$, on the assumption of the equality of the electromagnetic and weak vector currents. After excluding events outside the ρ peak, the experiment measures the branching ratio $b(\tau^- \to \rho^-\nu_\tau) = (20.5 \pm 4.1)\%$.

The majority of the single-prong decays of the τ have been measured and agree well with the theoretical calculations. The remaining one-prong modes are predicted to be predominantly final states of the type $\nu_\tau\pi^- \geq 2\pi^0$, and they form 10% of τ decays. The largest contributor is expected to be $\nu_\tau\pi^- 2\pi^0$, which should be comparable with $\nu_\tau\pi^-\pi^-\pi^+$. The latter mode has been

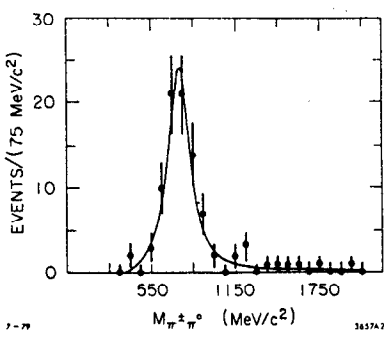

Fig. 8. The $\pi^-\pi^0$ invariant mass observed by Mark II for the decays $\tau^- \to \pi^-\pi^0\nu_\tau$.

isolated by the PLUTO detector at DORIS and a fairly detailed analysis of the small data sample has been recently completed.[10] The experimenters have selected events which contain only a lepton and three charged pions (with zero total charge). In order to suppress hadronic backgrounds, a missing-mass cut of at least 0.9 GeV/c^2 is required. There are 54 events which survive and the invariant masses of the two $\pi^+\pi^-$ combinations per event are plotted in Fig. 9. Most events indicate one combination consistent with ρ^0 and a study shows that non-resonant 3π production is < 32% (95% CL) of the total. The analysis proceeds by cutting about the ρ mass to give a sample of 27 signal and 13 background events. The invariant mass of the $\rho\pi$ system is compared with non-resonant (Fig. 10a) and resonant (Fig. 10b) spectra. A non-resonant s-wave $\{J^P(\rho\pi)=1^+\}$ can account for the observed spectrum whereas p- and d-waves show poorer agreement. An independent Dalitz plot study indicates $J^P=1^+$(s-wave) and $J^P=2^-$(p-wave) to be acceptable and other assignments to be at least an order-of-magnitude less likely. A resonant Breit-Wigner fit (Fig. 10b) assumes the values, M=1.0 GeV/c^2 and Γ=0.48 GeV/c^2. In summary, there is a definite signal of the decay $\tau^-\to\rho\pi^-\nu_\tau$ and the $\rho\pi^-$ state is probably $J^P=1^+$. The measured branching ratio of (5.4 ± 1.7)% is in accord with the theoretical estimate and shows that the 3π axial current is rather large, only a factor of two less than the 2π vector current. The present data is insufficient to determine whether a resonant structure is present in the 1^+, $\rho\pi$ system. However, it is likely that the Mark II experiment will be able to settle this question in the near future. The bizarre situation in which τ decays measure the parameters of the elusive A_1 meson was forcasted by Sakurai[11] in 1975!

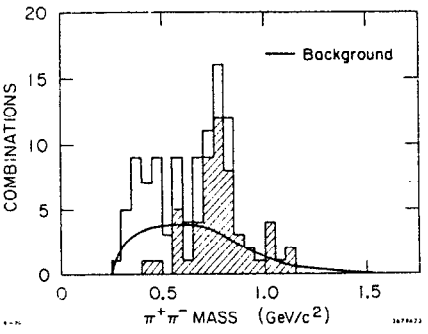

Fig. 9. The $\pi^+\pi^-$ mass spectrum observed by PLUTO in events containing only four prongs, $\pi^-\pi^-\pi^+$lepton$^+$. The higher mass combination in each event is indicated by the shaded histogram. The background of hadronic events with a misidentified lepton is shown by the solid curve.

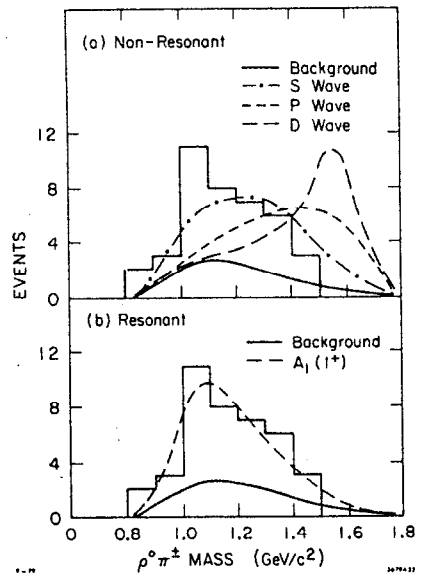

Fig. 10. The $\rho^0\pi^-$ mass spectrum measure by PLUTO. The fitted curves, which are superimposed over the background (solid curve), correspond to τ decays into a) a non-resonant $\rho\pi$ system for several values of the relative angular momentum and b) a 1^+ resonant $\rho\pi$ system of mass 1.0 GeV/c^2 and width 0.48 GeV/c^2.

There has only been one direct measurement of the inclusive multi-prong branching ratio of the τ which is free of the biases of charm decays. This has resulted from the DELCO observation, below charm threshold, of multi (≥ 3) prong events containing a single electron. These events display (Fig. 11) a rise in the energy range 3.50 - 3.72 GeV which is compatible with the τ. The observed events are corrected for backgrounds due to false electron tags. The corrections are large, e.g., the background-fraction in the observed events at 3.67 GeV is 60%. They are determined both by calculation and comparison with electron events observed at the ψ(3095). After accounting for systematic errors, the fit in Fig. 11 measures $2b_e b_{mp} = 0.098 \pm 0.022$, where b_{mp} is the τ multi-prong branching ratio. Using the world average experimental value of the electronic branching ratio, $b_e = 0.175 \pm 0.011$, determines $b_{mp} = 0.28 \pm 0.06$.

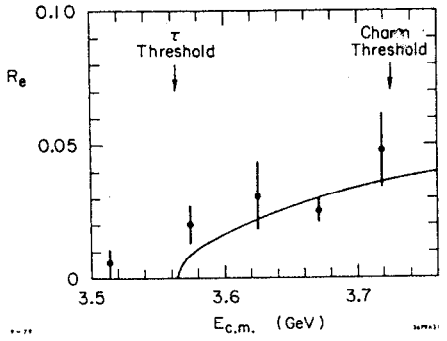

Fig. 11. The multi-prong electron cross-section ratio, $R_e=\sigma(e+\geq 2\text{-charged-particles})/\sigma_{\mu\mu}$ observed by DELCO below charm threshold, in the energy range, $3.50 < E_{cm} < 3.72$ GeV. The fitted curve (χ^2/dof = 4.5/3) indicates the threshold behavior of $\tau^+\tau^-$ pairs.

In summary, all experimental branching ratios or upper limits confirm, within their present precision, the predictions of the standard model. This model considers the τ^- and ν_τ to be a third weak iso-doublet lepton pair which joins the family previously comprised of $e^- - \nu_e$ and $\mu^- - \nu_\mu$. We will briefly consider alternative possibilities in the next section.

C. Lepton Classification

The experimental observations which we have discussed prove the existence of a new charged lepton which decays to final states involving an unobserved neutral particle. It is the nature of this neutral particle and of its coupling with the τ^- which classifies the new lepton. The experimental information which has been instrumental is:

1) The τ lifetime limit: $\tau_0 < 2.3\times10^{-12}$ sec (95% CL)

2) The branching ratio upper limit to three charged leptons of < 0.6% (90% CL)

3) The ratio of the muonic to electronic decay rate $b(\tau^-\to\mu^-\bar{\nu}_\mu\nu_\tau)/b(\tau^-\to e^-\bar{\nu}_e\nu_\tau) = 1.06 \pm 0.10$

4) The electron energy spectrum in the decay $\tau^-\to e^-\bar{\nu}_e\nu_\tau$, which indicates $\rho=0.72 \pm 0.15$ and $m_{\nu_\tau} < 250$ MeV/c^2

5) The absence of the reaction ν_μ + Nucleus $\to e^\pm X$,[12] where X contains no muons. This final state could result from $\tau^\pm X$ production and provides the experimental upper limit of 2.5% (90% CL) for the ratio of the $\nu_\mu - \tau$ coupling to the $\nu_\mu - \mu$ coupling

6) The precise limits on e - μ universality,[13] e.g., $b(\mu^-\to e^-\gamma) < 2.10^{-10}$ (90% CL), $b(\mu^-\to e^-e^-e^+) < 1.9\times 10^{-9}$, $\Gamma(\pi\to e\nu)/\Gamma(\pi\to\mu\nu) = (1.03 \pm .02) \times$ Theory.

The details of the comparison of the data with specific models, and their original references, are given by Gilman.[14] The following assignments for the neutral particle which participates in τ^- decays are excluded: $\bar{\nu}_e$, ν_μ, $\bar{\nu}_\mu$ and mixtures of ν_e and $\bar{\nu}_\mu$ in certain models, e.g., the heavy-neutrino (N_τ) model in which $m_{N_\tau} > m_\tau$. However, the assignment $\nu_\tau \equiv \bar{\nu}_e$ is not experimentally excluded, despite the upper limit of 2.6% for the branching ratio $\tau^- \to e^-\gamma$.

The simplest classification which remains is that of e - μ - τ universality in which each charged lepton couples via the same weak current to its own neutrino. Over the four years since the first indications of the τ, a broad range of its properties have been measured and together they provide persuasive evidence in support of this "standard model".

III. The Hadronic Cross-Section and Charmonium

A. QCD Predictions

The measurement of the cross-section, $\sigma(e^+e^- \to$ hadrons), provides direct tests of the only theory we have for the strong interactions: quantum chromodynamics (QCD). This model predicts the ratio of the hadronic cross-section to the μ-pair cross-section to be in zeroth order, $R_0(E_{cm}) = 3\sum_{i=1}^{N_f} Q_i^2$, where Q_i is the charge of the i^{th} quark and the sum is over the quarks with mass $\lesssim 0.5\ E_{cm}$. This expression follows from the assumption that hadronic events originate from quark-antiquark pair-production (Fig. 12a). The measurement of R therefore indicates the number of quarks and their charges, if they possess color and if they are point-like. In addition, by measuring the angular distribution of the "jet-axis" within the hadronic events, a test is made of the assumption that the quarks have $J = \frac{1}{2}$.

The theory of QCD also requires the existence of gluons, which influence the hadronic cross-section by means of gluonic radiative corrections. The first-order terms (Fig. 12b) introduce a correction to R of magnitude α_s/π. The quantity $\alpha_s (= g^2/4\pi)$ is the square of the strong coupling constant at the qqg vertex and has the value $12\pi/\{33-2N_f\} \ln s/\Lambda^2$. In this expression, N_f is the number of quark flavors and Λ a constant, which from lepton (e,μ,ν) scattering experiments is found to have a value near 0.5 GeV/c^2. The second-order corrections have only recently been calculated[15] and result in the theoretical

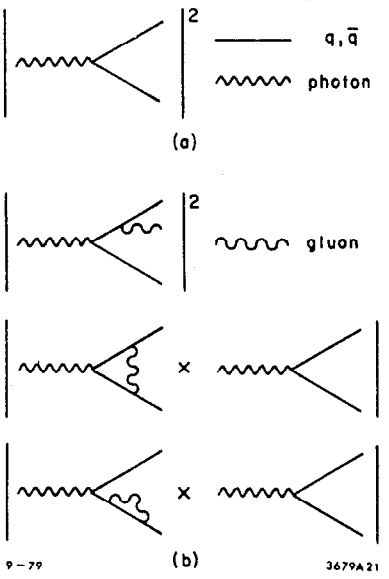

Fig. 12. The diagrams which are used to calculate a) the "bare" hadronic cross-section and b) the first-order corrections due to gluon radiation.

value,

$$R = R_0\{1 + \alpha_s/\pi + (1.98 - 0.12N_f)(\alpha_s/\pi)^2 + \ldots\}$$

The main predictions are as follows:

a) The first-order correction is large (~ 10%)

b) The second-order terms are small (~ 2%)

c) The value of R will slowly decrease with increasing q^2, assuming no quark thresholds are crossed. This is a consequence of the "running" coupling constant α_s.

In Fig. 13 a comparison is made of the QCD calculation of R with the Mark I measurements in the energy

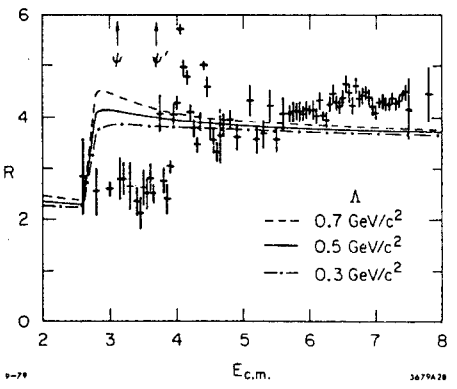

Fig. 13. The hadronic cross-section ratio, $R = \sigma(\text{hadrons})/\sigma_{\mu\mu}$, after radiative corrections and τ subtraction, as measured by Mark I. The error-bars do not include a systematic uncertainty of 15%. The curves show the QCD prediction for several values of the mass parameter Λ.

range, $2.6 < E_{cm} < 7.8$ GeV.[16] The curves include the limits of the uncertainty in the value of Λ, and the charmed quark threshold is chosen to accommodate the ψ and ψ' contributions. For energies above 5 GeV, which are beyond the resonance region, the measurements are higher than predictions by 10 - 15%. Since this is equal to the systematic precision of the measurement there is no conflict with the theoretical curve.

It has been stressed by Bjorken[17] and others that the measurement of R is a "gold-plated" test of QCD. In contrast with most applications of the theory, this calculation does not suffer from illnesses such as large non-leading corrections and is applied to a "well understood" quark-antiquark system. However, all present measurements have been limited to a 10-15% accuracy by systematic effects, whereas about 2% accuracy is required to test QCD. The systematic errors are due to uncertainties in the detection efficiencies, background subtractions of 2γ, τ, beam gas, cosmics and QED processes, and radiative corrections. An ideal apparatus, which avoids many of the systematics faced by the present detectors, is a calorimeter with a large-solid-angle measurement of both charged and neutral particles and with the ability to trigger on a deposited energy which is a small fraction of the center-of-mass energy. A possible candidate would be the Crystal Ball surrounded by a large, totally active liquid-scintillator hadron calorimeter.

In common with most QCD caculations, the prediction for the hadronic cross-section does not account for resonances. However, the charmonium resonances, which are observed near charm threshold, provide a unique opportunity to explore the QCD features of a bound system of two quarks which are non-relativistic and therefore "calculable". The experimental status of the charmonium states is summarized in the next section.

B. Charmonium

Charmonium levels are characterized in the spectroscopic notation, $n^{2S+1}L_J$ where n is the principal quantum number (or radial excitation number), S(= 0 or 1) is the sum of the quark and antiquark spins, L their relative orbital angular momentum and J the total spin of the system. States with J = 1 appear as s-channel resonances in the hadronic cross-section (Table III).

Table III. Charmonium States† Observed as Resonances in the Hadronic Cross-Section

S	L	J^{PC}	$^{2S+1}L_J$	n	Name	Mass (MeV/c^2)
1	0	1^{--}	$^3S_1$	1	J/ψ	3097 ± 2
				2	ψ'	3686 ± 3
				3	ψ	4028 ± 5
				4	ψ	4414 ± 7
1	2	1^{--}	$^3D_1$	1	ψ''	3768 ± 4
				2	ψ	4160 ± 20

† The spectroscopic assignments are those favored by the theory.[18]

A comparison of the experimental measurements[19] (Fig. 14) of the hadronic cross-section near charm threshold indicates the following:

a) Clear establishment of peaks at 3.77 GeV and 4.03 GeV and a fair agreement on the shape of the structure at 4.4 GeV (although this appears exceptionally pronounced in the Mark I data).

b) Disagreement on the presence or significance of a peak at 4.16 GeV.

c) Possible structure in the region near 3.95 GeV.

d) Agreement within the systematic errors on the magnitudes of the cross-section before and after charm threshold. (In fact, a comparison of these plots provides a yardstick for the present systematic precision of the experimental value for R.)

A large part of the discrepancy which exists at 4.16 GeV can be explained by radiative corrections. These require as input the structure seen in the raw data and this structure is exaggerated after the application of radiative corrections. Typically, in this region, a peak will be increased by 10% and a dip decreased by about 10%. The 4→4.2 GeV region has not been measured with high precision and could possibly be far more complicated than presently interpreted. The moral is that future measurements of R should show the raw data both before and after radiative corrections.

The low-lying charmonium states, for which $J^{PC}\neq 1^{--}$, have been explored by measuring the radiative decays of the ψ and ψ' (Table IV). Since a detailed presentation is made at this conference of the status of the radiative charmonium levels, I will restrict myself to a few brief comments. The major progress has been the exclusion of the possible pseudoscalars at masses 2820, 3450 and 3590 MeV/c^2 (to the great relief of charmonium theorists!) and the contribution of a new η_c candidate, from the Crystal Ball, at a mass of 2980 MeV/c^2.[20] The most striking absence occurs when comparing the Crystal Ball data[21] with the signal expected from DASP enhancement at 2820 MeV/c^2 (Fig. 15). In summary, the levels which could not be accommodated into the charmonium model have been experimentally excluded and a promising candidate for the lowest-mass pseudoscalar $c\bar{c}$ state has been observed.

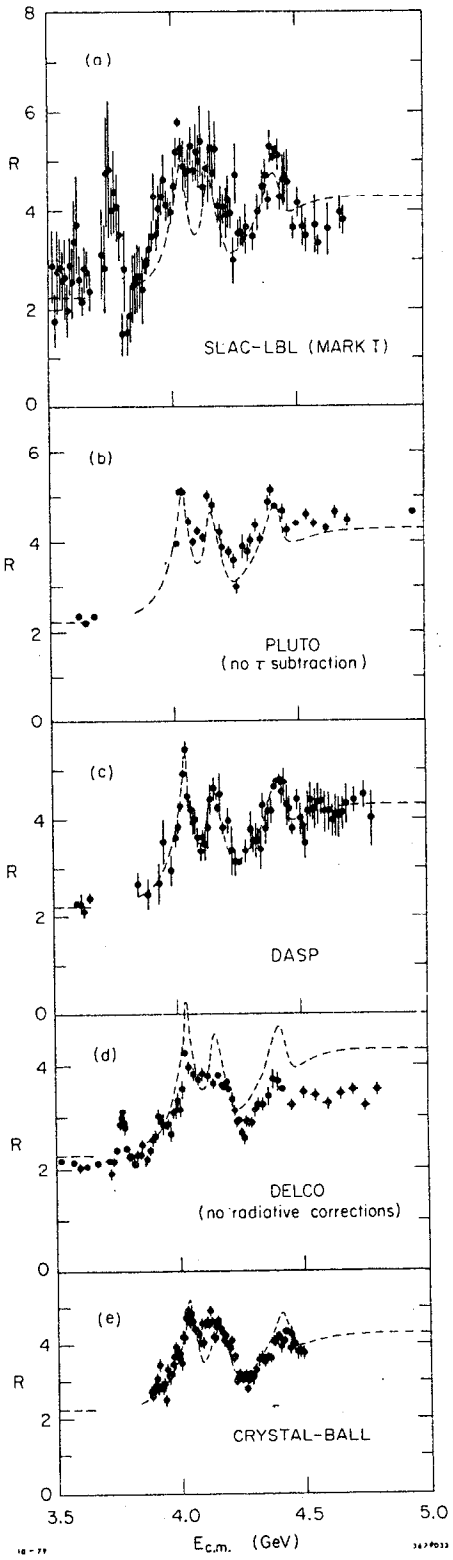

Fig. 14. The observed values of R near charm threshold. All data are corrected for radiative effects and contamination from the τ, unless otherwise indicated. The hand-drawn curve, which follows the DASP points, has been applied to the other measurements in order to facilitate a comparison. Systematic errors, which range from 10-15%, are not included in the error-bars.

Table IV. Charmonium States Observed in ψ and ψ' Radiative Decays

S	L	J^{PC}	$^{2S+1}L_J$	n	Name	Mass (MeV/c^2)
0	0	0^{-+}	$^1S_0$	1	η_c	(2820), 2980 ± 30
				2	η_c'	(3450), (3590)
1	1	0^{++}	$^3P_0$	1	χ	3412 ± 2
		1^{++}	$^3P_1$	1	χ	3507 ± 3
		2^{++}	$^3P_2$	1	χ	3551 ± 3
0	1	1^{+-}	$^1P_1$	1		not seen

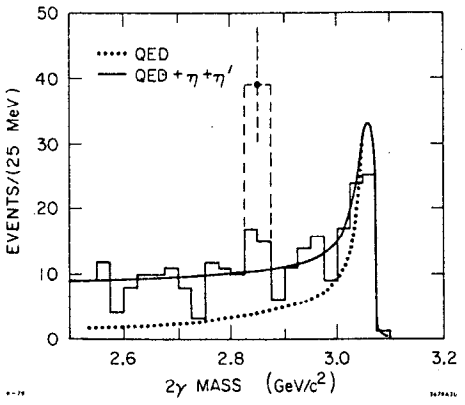

Fig. 15. The 2γ mass spectrum (high solution) observed by the Crystal Ball in the decays $\psi \to \gamma\gamma\gamma$. The curves show the contributions expected from the sources $\psi \to \eta\gamma$, $\eta'\gamma$ and QED 3γ. The dashed histogram indicates the signal expected from the DASP candidate for a pseudoscalar state (which is conservatively shifted to 2850 MeV/c^2).

select events of the type $\gamma\gamma$ + ≥ 2-charged-particles + anything, in which the two photons must each exceed 140 MeV and have the vector sum of their momenta lie between 0.3 and 1.4 GeV/c. The 2γ-invariant-mass is measured at several energies (Fig. 16) and shows a clear π^0 peak superimposed over a smooth background due to false combinations. The shape of the combinatorial background is determined both by Monte Carlo calculation and by combining photons from different events. The data also shows an excess of events in the η mass region at 4.42 GeV, but no compelling evidence for η production at other energies. This is particularly true at 4.03 GeV where the upper limit is measured for η production in D decays, $b(D \to \eta X) < 2\%$. On this basis it is argued that the η source at 4.42 GeV is neither D's nor "old physics". The η signal is small: (4.1 ± 0.9)nb or approximately 10% relative to π^0 production. This analysis requires a careful understanding of the background shape, which results from a raw spectrum that increases rapidly at low masses and a detection efficiency with the opposite behavior.

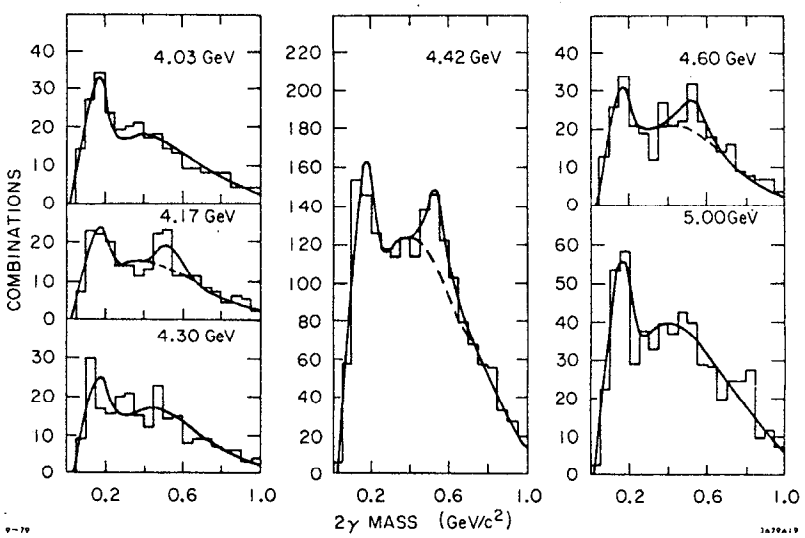

Fig. 16. The 2γ mass distribution observed by DASP at several center-of-mass energies in events of the type 2γ + ≥ 2-charged particles + anything. The smooth lines account for combinatorial backgrounds, π^0 and, at certain energies, η production.

IV. The F Mesons

A. General Properties

Since the F mesons are built of a charmed and strange quark, they will decay strongly to a DK final state for $m_F > 2360$ MeV/c^2. Experimentally, the ground state (pseudoscalar) F particle is below this mass so we expect it to decay weakly to states which include $s\bar{s}$: $K\bar{K}X$ (X = nπ, eν, μν), φX, ηX and η'X. The vector version of this particle, the F^*, cannot decay strongly to Fπ since it would violate isospin. Since it appears that $m_{F^*} < m_F + 2\pi$, we expect the decay $F^* \to F\gamma$ to account for essentially the full decay rate.

These characteristics have been exploited in searching for F production in e^+e^- annihilation. As we shall see in the following section, there is very sparse experimental information presently available.

B. Experimental Status

The only evidence which supports the presence of F's has been presented by DASP.[22] The experimenters

When a further requirement is imposed that there be an additional photon of energy less than 140 MeV, the data (Fig. 17) suggests a possible enhancement of the η peak at 4.42 GeV. Again the background knowledge is crucial. (In these plots the solid lines are estimates of the uncorrelated photon backgrounds, normalized to the data with $m_{\gamma\gamma} > 0.7$ GeV/c^2.)

As a result of these inclusive observations, the DASP group restricts their attention to events of the type $\pi^\pm + \gamma\gamma + \gamma_\ell + X$, where the pion momentum exceeds 0.6 GeV/c, the γγ mass lies within the η band and the energy of γ_ℓ is below 140 MeV. The events are fitted to the reaction $e^+e^- \to F^\pm F^{*\mp} \to (\pi^\pm\eta)(F^\mp\gamma_\ell)$, with the constraint that the $\pi^\pm\eta$ mass equal the $F^\mp$ (recoil) mass. The events which have an acceptable fit to this hypothesis are plotted in Fig. 18. The data at 4.42 GeV shows a peak of six events at $m_{\pi\eta} = m_F = 2.04 \pm 0.02$ GeV/c^2, whereas the data at other energies, which provides a control sample, shows no such peak. By measuring the photon energy associated with the six signal events, the F^* mass is found to be $m_{F^*} = (2.15 \pm 0.05)$ GeV/c^2. Finally, on the assumption that all the inclusive η's at 4.42 GeV are due to F decay, the relative rate $\Gamma(F \to \pi\eta)/\Gamma(F \to \eta X)$ is found to be 0.09 ± 0.06.

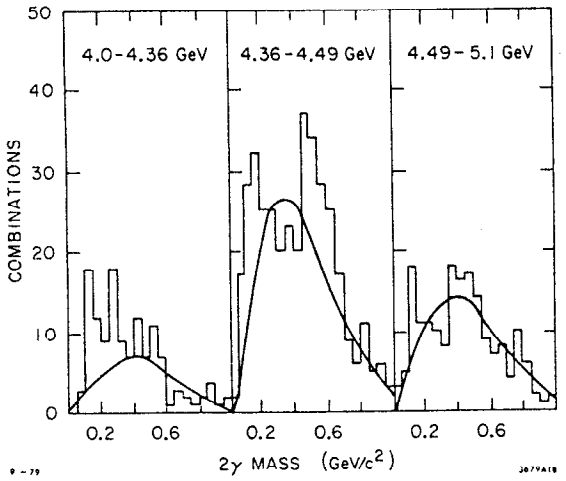

Fig. 17. The data of Fig. 16 after imposing the requirement of an extra photon below 140 MeV. The solid lines indicate the expected combinatorial backgrounds.

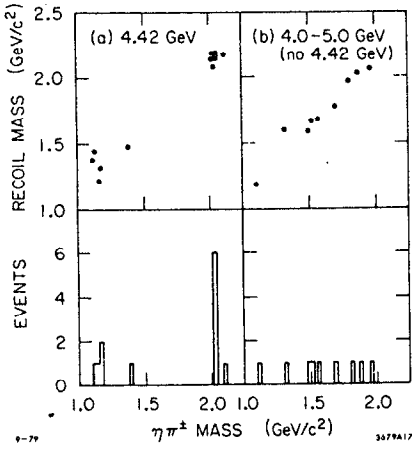

Fig. 18. The DASP evidence for $F\bar{F}^*$ production based on fits to events of the type $\pi^{\pm}\eta + X\gamma$, where the mass of the recoil particle, X, is constrained to be equal to the $\pi^{\pm}\eta$ mass.

There is very little information about F's from other experiments. A possible peak in the $K\bar{K}n\pi$ mass system at 2.04 GeV/c^2, observed by the LGW experiment, has been ruled out by Mark II measurements at a higher sensitivity. The Mark II apparatus is not suited to a measurement of inclusive η's but it is possible that the Crystal Ball will be able to provide an independent check of the DASP η measurements. The Mark II detector finds[23] upper limits for F production which are close to the positive result from DASP (Table V).

Table V. Mark II Cross-Section Upper Limits for F Production

Decay Channel	E_{cm} (GeV)	σ_FxBR (95% CL)
$F^+ \to \pi^+\eta$	4.16	< 0.33 nb
	4.42	< 0.26 nb*
$F^+ \to K^+\bar{K}^0$	4.16	< 0.13 nb
	4.42	< 0.22 nb

*c.f. DASP result: 0.41 ± 0.18 nb

The F's are certainly the most poorly-understood of the ground-state charmed particles. It will be an important goal of future e^+e^- measurements to provide independent support of the DASP data and to measure the F properties.

V. The Charmed Baryons

A. General Properties and Observations at Proton Accelerators

The lowest charmed baryon states are made of u, d and c quarks with zero relative orbital angular momentum of all pairs. The lightest is the spin ½ Λ_c^+ (udc with ud in an I = 0, S = 0 state) followed by the spin ½ $\Sigma_c^{o,+,++}$ (ddc, udc and uuc, respectively, with "ud" in an I = 1, S = 1 state) and finally the spin 3/2 $\Sigma_c^{*o,+,++}$. Since the mass of the Λ_c^+ is less than $m_N + m_D$, it decays weakly to states such as NKX (X = nπ, eν, μν), ΛX, ΣX, etc. If the masses of the Σ_c's exceed $m_{\Lambda_c} + m_\pi$ then these states will predominantly decay down to the Λ_c^+ by pion emission.

In contrast with the situation for charmed mesons, e^+e^- storage rings have come second to proton accelerators in the observation of charmed baryons. In the last few months there has been a dramatic growth in the number of experiments which have seen charmed baryon signals. I have attempted to summarize the relevant data from proton accelerators in Table VI.

Table VI. Summary of Observations of Charmed Baryons at Proton Accelerators

Experiment	Reference	Production	Decay Channel	Mass (MeV/c^2)
BNL 7' BC (COL-BNL)	24	$\nu_\mu p$	$\Lambda\pi^+\pi^+\pi^+\pi^-$	2426 ± 12
		$\nu_\mu p$	$\Lambda\pi^+\pi^+\pi^-$	2260 ± 20
		$\nu_\mu d$	$K_s^o\pi^-\pi^+p$	2254 ± 12
FNAL Photo-production (CIHF)	25	γN	$\bar{\Lambda}\pi^+\pi^-\pi^-$	2260 ± 20
FNAL 15' BC I (COL-BNL)	26	$\nu_\mu N$	$K_s^o p, \Lambda\pi^+$	2257 ± 10
FNAL 15' BC II (TIMST)	26	$\nu_\mu d$	$\Lambda\pi^+\pi^+\pi^-$	2257 ± 17
BEBC Emulsion (ABCDLOPRT)	26	$\nu_\mu N$	$K^-\pi^+p$	2295 ± 15
ISR I (UCLA-SACLAY)	27	pp	$K^-\pi^+p$	2290 ± 11
ISR II (ACHMNR)	27	pp	$K^-\pi^+p$	2262 ± 10
ISR III (ACCDHW)	27	pp	$K^-\pi^+p$	2260 ± ?

Much of this data is unpublished and preliminary, and may eventually change. However, it is instructive to try to group the ten mass measurements: seven are consistent with an average mass of 2259 ± 6 MeV/c^2, two show an average mass of 2292 ± 9 MeV/c^2 and one measurement is at 2426 ± 12 MeV/c^2. The final measurement is presently interpreted as a candidate for either the Σ_c^{++} or the Σ_c^{*++}, which is observed to decay by pion emission to the Λ_c^+. From the mass splittings of the lighter baryons (Σ and Λ) it is unlikely that there is more than one state between 2.25 and 2.30 GeV/c^2, so the most favored Λ_c^+ mass is 2.26 GeV/c^2. We will now turn our attention to the e^+e^- data on this subject.

B. Inclusive Baryon Production

Until recently, the only evidence for charmed baryons in e^+e^- annihilation came from the measurement of inclusive baryon production. The Mark II measurements of the inclusive proton and Λ cross-sections as a function of E_{cm} [28] are shown in Fig. 19. The quantities displayed are $R(p+\bar{p}) = 2\sigma(\bar{p})/\sigma_{\mu\mu}$ and $R(\Lambda+\bar{\Lambda}) = \{\sigma(\Lambda)+\sigma(\bar{\Lambda})\}/\sigma_{\mu\mu}$, where the former measurement avoids the large backgrounds due to beam-gas interactions. Both channels display a sharp increase in cross-section near 4.5 GeV, coincident with the kinematic threshold for charmed baryon production. These effects are clearly imcompatible with the naked charm threshold or the gentle logarithmic dependence expected with increasing energy. The observed step sizes of 0.31 ± 0.06 and 0.10 ± 0.03 for $p+\bar{p}$ and $\Lambda+\bar{\Lambda}$, respectively, [29] indicate the Λ/p fraction in charmed baryon decays is $(41\pm15)\%$, after excluding the protons from Λ decays. This measurement applies to the Λ_c^+, since most heavier charmed baryons probably cascade down to the Λ_c^+.

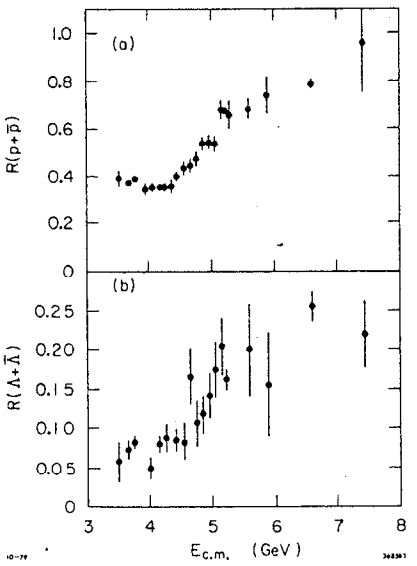

Fig. 19. The Mark II measurements of the inclusive cross-section ratios for a) $p+\bar{p}$ and b) $\Lambda+\bar{\Lambda}$ as a function of center-of-mass energy. The error-bars do not include overall systematic errors of a) 17% and b) 27%, which may vary slowly with energy.

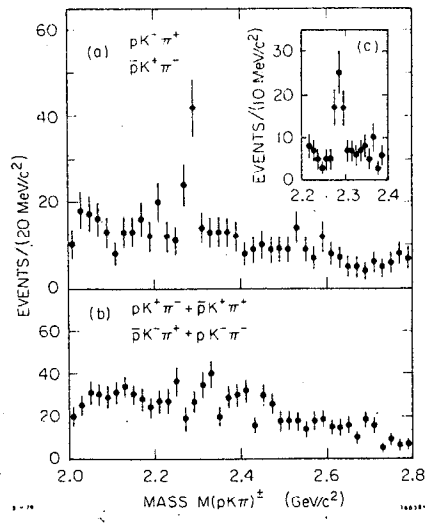

Fig. 20. The pKπ mass distributions measured by Mark II above $E_{cm} = 4.5$ GeV for a) charge combinations with the quantum numbers of the $\Lambda_c^\pm$ and b) charge combinations incompatible with the $\Lambda_c^\pm$. The inset c) shows, in finer binning, the enhancement observed at (2285 ± 6) MeV/c^2.

C. Resonance Characteristics

The conclusive evidence for charmed baryon production in e^+e^- annihilation was provided recently by the Mark II observation[28] of a peak in the $K^-\pi^+p$ mass spectrum (Fig. 20a) for data taken above $E_{cm} = 4.5$ GeV. The smooth background is measured both in shape and magnitude by taking the combinations $K^+\pi^-p$ and $K^+\pi^+\bar{p}$ (fig. 20b) and dividing the result by two. After accounting for systematic errors, the peak is found to occur at a mass of (2285 ± 6) MeV/c^2. This is naturally interpreted as the Λ_c^+, but the observed mass lies above most of the measurements in Table VI. Since it is unlikely that two states are involved, the discrepancy is probably due to unaccounted systematic errors in the measurements.

The signal is found to have the magnitude, $\sigma(\Lambda_c+\bar{\Lambda}_c)\ b(\Lambda_c\to K\pi p) = (0.037\pm0.012)$ nb. This can be translated into a branching ratio measurement by attributing the rise in $\sigma(p+\bar{p})$ solely to the Λ_c^+, whereby, $\sigma(\Lambda_c+\bar{\Lambda}_c) = \Delta R(p+\bar{p})\ \sigma_{\mu\mu}/0.6 = (1.7\pm0.4)$ nb. The factor 0.6 accounts for a statistical estimation of the ratio $p/(p+n)$ in Λ_c^+ decays. The result is the branching ratio, $b(\Lambda_c^+\to K^-\pi^+p) = (2.2\pm1.0)\%$.

There have been some preliminary studies made of resonance formation in the Kπp system and of other decays of the Λ_c^+. After subtracting the non-resonant background, the $\bar{K}^{*0}p/K^-\pi^+p$ fraction is found to be $(12\pm7)\%$ and the $K^-\Delta^{++}(1236)/K^-\pi^+p$ fraction is $(17\pm7)\%$. A positive signal is found for $\bar{K}^0p/K^-\pi^+p$ (0.8 ± 0.4) and and upper limits of 0.75(95% CL) and 0.8 (95% CL) are placed on the ratios $\Lambda\pi^+/K^-\pi^+p$ and $\Lambda\pi^+\pi^+\pi^-/K^-\pi^+p$, respectively.

The existence of charmed baryons is now well established and we can look forward in the near future to a marked increase in our knowledge of their properties.

VI. The D Mesons

A. General Properties

The SLAC-LBL measurements of the masses of the ground-state pseudoscalar and vector D mesons are summarized in Table VII. Despite the large Q values

Table VII. The Masses of the Ground-State D Mesons

S	L	J^P	Composition	Name	Mass (MeV/c^2)
0	0	0^-	$c\bar{u}$	D^0	1863.3 ± 0.9
			$\bar{c}d$	D^+	1868.3 ± 0.9
1	0	1^-	$c\bar{u}$	D^{*0}	2006.0 ± 1.5
			$\bar{c}d$	D^{*+}	2008.6 ± 1.0

involved in the decays, these masses have been determined precisely in e^+e^- collisions. The techniques are described by Feldman[30] along with a discussion of the experimental data which supports the spin-parity assignments for the D and D^*. An example is the angular distribution of $D\bar{D}$ pairs observed at the ψ'' (Fig. 21) which shows a $\sin^2\theta$ dependence, as expected for spin 0 particles.

The same group has measured the D^* branching ratios (Table VIII). The results are derived[30] from a combination of theoretical assumptions and fits to the D^0 and D^+ momenta observed at $E_{cm} = 4.03$ GeV (Fig. 22). It is worthwhile keeping in mind that these branching ratios are obtained rather indirectly and so an independent measurement is desirable. This may be available in the near future by a direct measurement in the Crystal Ball of the π^0 and γ yield at $E_{cm} = 4.03$ GeV.

B. Inclusive D Production

A SLAC-LBL measurement of D production throughout this energy range has recently been completed.[31] The results are displayed in Fig. 23 along with a curve which indicates the charm cross-section, derived from the total hadronic cross-section after subtracting "old physics". The curve closely follows the D cross-section and in particular confirms, within 15% accuracy,

Fig. 21. The polar angular distribution of $D\bar{D}$ pairs observed by SLAC-LBL at the ψ''. The fitted value of α in the function $1+\alpha\cos^2\theta$ is found to be a) -1.00 ± 0.09 and b) -1.04 ± 0.10.

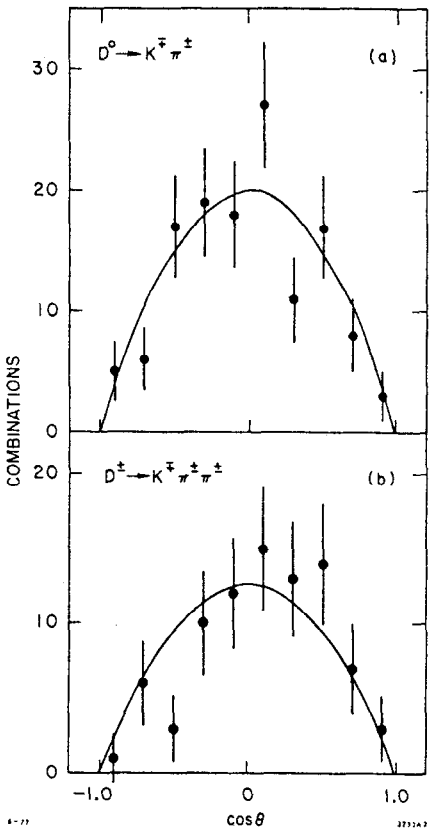

that the ψ'' decays only to $D\bar{D}$ final states. This is reassuring since much of our quantitative knowledge of the D's is obtained at the ψ''.

The measurements also indicate that D's probably dominate the charm cross-section at all energies. We will combine some previous information to obtain the relative $D:F:\Lambda_c$ production rate in e^+e^- annihilations since it may be a useful yardstick for estimations of charmed particle cross-sections in other processes. At $E_{cm} = 5.2$ GeV, the total charm cross-section is $R_c = 1.6 \pm 0.3$ (Mark II) and so the Λ_c fraction is $0.5\ \Delta R(p+\bar{p})/0.6\ R_c = 0.15 \pm 0.04$. From the DASP inclusive η signal at 4.4 GeV we can estimate the lower limit for the F fraction to be $0.5\ \sigma_\eta / \sigma_{CHARM} = 0.5 \times (4.1 \pm 0.9)/11.3 = 0.18 \pm 0.04$. At 5.0 GeV, DASP sees no η signal and sets a 2σ upper limit σ_η (5 GeV)< 1.6 nb. The general picture which emerges is that the ratio $D:F:\Lambda_c$ is of the order 3:1:1, which partly explains the chronological sequence of the discovery of these particles.

Table VIII. The D^* Branching Ratios

Mode	Branching Ratio (%)
$D^{*0} \to D^0\pi^0$	55 ± 15
$D^0\gamma$	45 ± 15
$D^{*+} \to D^0\pi^+$	64 ± 11
$D^+\pi^0$	28 ± 9
$D^+\gamma$	8 ± 7

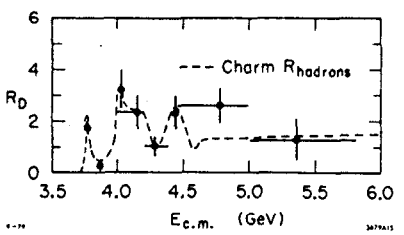

Fig. 23. The inclusive D cross-section ratio $R = \sigma(D^0+\bar{D}^0+D^+ + D^-)/2\,\sigma_{\mu\mu}$ measured by SLAC-LBL. The factor of 2 accounts for the pair production of D's and allows a direct comparison with the total charm (hadronic) cross-section (dashed curve) measured in the same experiment.

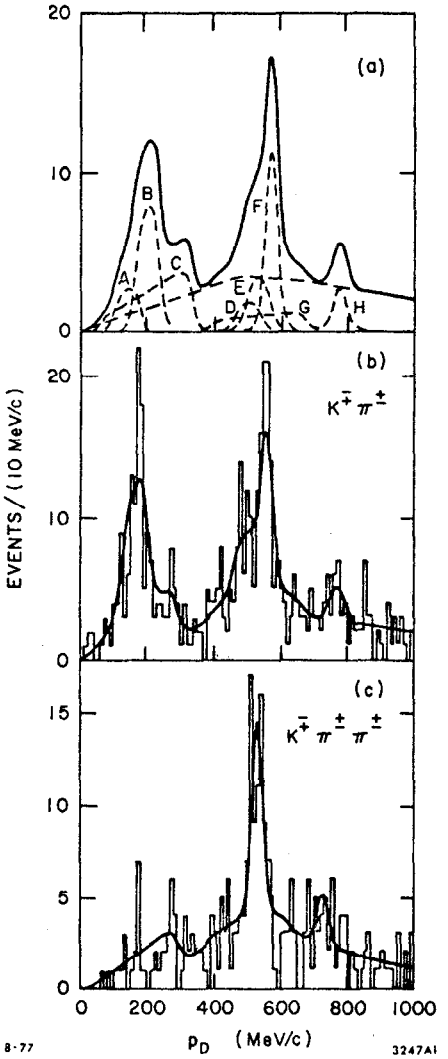

Fig. 22. The D momenta spectra measured by SLAC-LBL at 4.03 GeV for b) $D^0 \to K^-\pi^+$ and c) $D^+ \to K^-\pi^+\pi^+$. The solid curves represent the fits to the data and the dashed curves in a) indicate the individual contributions (detailed in Ref. 30). The three peaks around 200, 500 and 750 MeV/c correspond to production of $D^*\bar{D}$, $D^*\bar{D}$ and $D\bar{D}$, respectively.

C. General Features of D Decays

The original LGW measurement[33] of the inclusive prong distributions in D^0 and D^+ decays has been verified with greater precision in a preliminary Mark II analysis[32] (Fig. 24). In the new data, the mean charged multiplicities are 2.46 ± 0.14 and 2.16 ± 0.16 for D^0 and D^+, respectively.

These measurements are made at the ψ'' in events containing a tagged $D^0(K^-\pi^+$ and $K^-\pi^+\pi^+\pi^-)$ or $D^+(K^-\pi^+\pi^+)$. The tagged events also provide information on the branching ratios to inclusive kaons and to exclusive final states. The inclusive kaon branching ratios measured by LGW[33] and Mark II[32] are summarized in Table IX.

It is interesting to note that both measurements fail, by 1.5 - 2σ, to account for all the D^+ decays, even after including in the tally the 5% contribution from Cabibbo-suppressed ($K \to \pi$) channels. However, the effect may simply result from a common

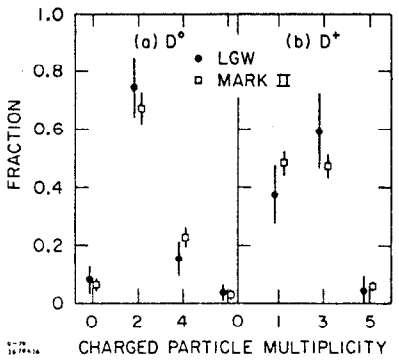

Fig. 24. The charged-particle multiplicity measured by LGW and Mark II for a) D^0 and b) D^+ decays. The data has been corrected for detection efficiencies.

Table IX. The Inclusive Branching Ratios, b(D→KX)

Mode	LGW (%)	Mark II (%) (preliminary)	Average (%)
$D^0 \to K^-$	35 ± 10	56 ± 5.6	50 ± 5
K^+		7.9 ± 2.6	7.9 ± 3
$\overline{K^0}^\dagger$	57 ± 26	20 ± 8.5	24 ± 8
Total	92 ± 28	84 ± 11	82 ± 10
$D^+ \to K^-$	10 ± 7	17 ± 4.1	15 ± 4
K^+	6 ± 6	5.6 ± 2.9	5.7 ± 3
$\overline{K^0}^\dagger$	39 ± 29	44 ± 15	43 ± 14
Total	55 ± 30	67 ± 16	64 ± 15

†Derived from the measurements of $K_S^0 \to \pi^+\pi^-$, after correcting by the branching ratio and assuming $\Gamma(\overline{K^0}) = 2\Gamma(K_S^0)$.

misunderstanding in K detection efficiencies, since the totals of the measured branching ratios are compatible, in all cases, with 80%. The most significant result is the observation by Mark II of the "wrong strangeness" decays D^0, $D^+ \to K^+$ at a level consistent with that expected from Cabibbo suppression. Both experiments find a rather low branching ratio for $D^+ \to K^-X$ which is in part a consequence of the semi-leptonic decay characteristics.

D. Hadronic D Decays

The LGW[34] and Mark II[32] experiments have measured the branching ratios of several exclusive D decays which involve $\leq 1\pi^0$. The "grist for the mill" is summarized in Table X. These modes only account for approximately 20% of the D^0 and D^+ decay channels. The remainder are largely semi-leptonic decays or hadronic decays including at least $2\pi^0$'s, which are very difficult to handle experimentally. At present there is only sketchy information concerning resonance (K^*,ρ) production in D decays. Since it bears on $D^\pm$ selection procedures which have been applied in certain experiments, we comment that there is very little (< 15%) indication of $\bar{K}^{*0}$ production in $D^+ \to K^-\pi^+\pi^+$. Hopefully, the situation will be clarified soon by Mark II.[32]

It is expected that the charm branching ratio measurements will improve our understanding of

Table X. The Exclusive Hadronic D Branching Ratios

Mode	LGW (%)	Mark II (%) (Preliminary)	Average (%)
$D^0 \to K^-\pi^+$	2.2 ± 0.6	2.8 ± 0.5	2.6 ± 0.4
K^-K^+		0.31 ± 0.09	0.31 ± 0.09
$\pi^-\pi^+$		0.09 ± 0.04	0.09 ± 0.04
$\overline{K^0}\pi^0$		2.1 ± 0.9	2.1 ± 0.9
$\overline{K^0}\pi^+\pi^-$	4.0 ± 1.3	2.7 ± 0.7	3.0 ± 0.6
$K^-\pi^+\pi^0$	12.0 ± 6.0	6.3 ± 2.2	7.0 ± 2.1
$K^-\pi^+\pi^+\pi^-$	3.2 ± 1.1	6.7 ± 1.4	4.5 ± 0.9
Total			19.6 ± 2.6
$D^+ \to \overline{K^0}\pi^+$	1.5 ± 0.6	2.1 ± 0.5	1.9 ± 0.4
$\overline{K^0}K^+$		0.5 ± 0.3	0.5 ± 0.3
$K^-\pi^+\pi^+$	3.9 ± 1.0	5.2 ± 1.0	4.6 ± 0.7
$\overline{K^0}\pi^+\pi^0$		16.4 ± 9.5	16.4 ± 9.5
$\overline{K^0}\pi^+\pi^+\pi^-$		5.1 ± 2.0	5.1 ± 2.0
$K^-\pi^+\pi^+\pi^+\pi^-$		< 2.0 (90% CL)	< 2.0 (90% CL)
Total			28.5 ± 9.7

non-leptonic weak interactions. The situation is, however, complicated by the existence of several decay mechanisms and by the uncertainties of final-state interactions. For a comparison with theoretical calculations it is particularly important to know the D^0 and D^+ lifetimes so that the experimental branching ratios can be converted into rates. This will be discussed later.

Presumably the simplest hadronic decays, which involve only two final particles, will provide the most useful information. The Mark II experiment has recently observed[35] the Cabibbo-suppressed decays $D^0 \to \pi^-\pi^+$ and $D^0 \to K^-K^+$ (Fig. 25). They measure the following

Fig. 25. The invariant mass distributions measured by Mark II at the ψ'' for a) $\pi^-\pi^+$ b) $K^-\pi^+$ and c) K^-K^+. The peaks at 1863 MeV/c^2 indicate D^0 decays with correct particle identification whereas the satellite peaks are due to one misidentified particle in the decay $D^0 \to K^-\pi^+$.

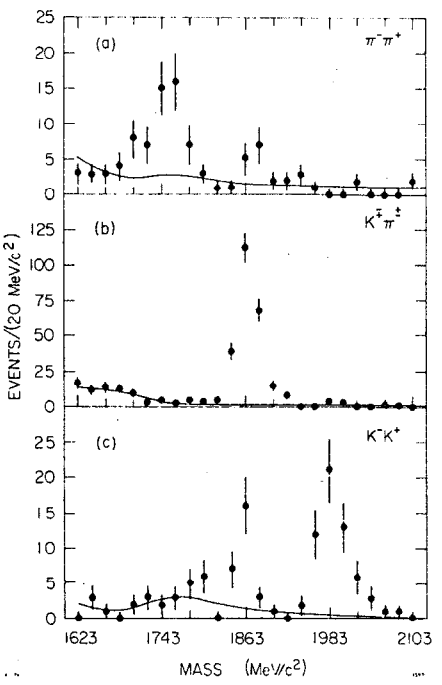

relative decay rates: $\Gamma(D^0 \to \pi^-\pi^+)/\Gamma(D^0 \to K^-\pi^+) = 0.033 \pm 0.015$ and $\Gamma(D^0 \to K^-K^+)/\Gamma(D^0 \to K^-\pi^+) = 0.113 \pm 0.030$. These are to be compared with the "naive" theory[36] which indicates the relative rates, $\tan^2\theta_c \times 1.07$ (phase-space) $= 0.054$ and $\tan^2\theta_c \times 0.92 = 0.046$ for $\pi^-\pi^+$ and K^-K^+, respectively. The discrepancy can be readily accommodated by a slight complication of the theory.[37] It is unfortunate that these beautiful measurements are unable to determine the Cabibbo angle in charm decays, but simply confirm it has roughly the expected magnitude.

E. Semi-Leptonic D Decays

In contrast with the situation for hadronic decays, tests of the charm current are relatively clean in semi-leptonic processes, since the hadronic current appears once and is multiplied by a known leptonic current.

Experimentally, the process $c \to se^+\nu_e$ is investigated by studying the multi-prong electron events, $e^\pm$ + ≥ 2-charged particles, which are chosen to minimize the τ background. The cross-section ratio of the charm multi-prong electron events, R_e^c, is seen in the DELCO data (Fig. 26) to follow the structure which is

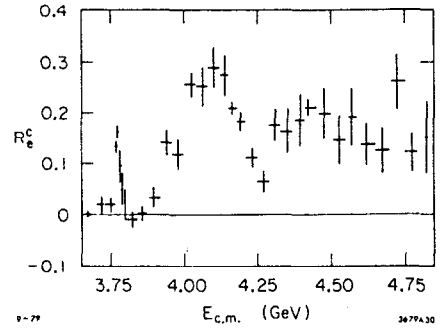

Fig. 26. The charm multi-prong electron cross-section, $R_e^c = \sigma(e^\pm + \geq 2\text{-charged-particles})/\sigma_{\mu\mu}$, in the energy range, 3.67 - 4.80 GeV. The data, recorded by DELCO, is corrected for backgrounds due to the τ and misidentified hadronic events. The error bars are statistical and do not reflect possible smooth energy-dependent systematic errors of 15%.

familiar from the hadronic cross-section. A direct comparison with the total charm cross-section is illustrated in Fig. 27, where the quantity R_e^c / R^c is plotted. The charm hadronic cross-section R^c is obtained in the same experiment by subtraction from the R plot of the (constant) "old physics" events as well as backgrounds such as the τ, ψ and ψ' radiative tails, 2-photon-process and beam-gas interactions. Since

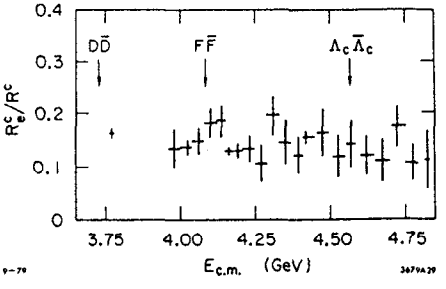

Fig. 27. The ratio of R_e^c to the total charm hadronic cross section, R^c, measured by DELCO. The ratio R_e^c/R^c is equal to $2\,b_e(1-b_e)$, where the branching ratio, $b_e = b(\text{charm} \to e\nu X)$.

Fig. 27 excludes events with 2 detected electrons, it measures the quantity $2b_e(1-b_e)$, where $b_e = \Gamma(\text{charm} \to e\nu X)/\Gamma(\text{charm} \to \text{all})$. In this context, "charm" is a varying mixture of D's, F's and Λ_c's whose composition is only known with any confidence at the ψ". For this reason, it is difficult at present to draw any firm conclusions from Fig. 27. However, taken at face value, b_e is consistent with being constant above 4 GeV and slightly higher at the ψ". Since no variation is observed at the F and Λ_c thresholds, these particles may have semi-leptonic branching ratios comparable with the D's although of course their electron contribution is diluted.

The measurements of the branching ratio, $D \to e\nu X$, are summarized in Table XI.

Table XI. The Branching Ratio for $D \to e\nu X$

Experiment	Reference	E_{cm} (GeV)	Branching Ratio (%)
DASP	38	3.99 → 4.08	8.0 ± 2.0
LGW	34	ψ"	7.2 ± 2.8
DELCO	39	ψ"	8.0 ± 1.5
MARK II	32	ψ"	10.0 ± 4.0
		Average	8.0 ± 1.1

In order to avoid the unknown contributions from other charm sources, these measurements are restricted to $E_{cm} < 4.08$ GeV. The composition of the "D" is (56 ± 3)% D^0 and (44 ± 3)% D^+ at the ψ" and (70 ± 10)% D^0 and (30 ± 10)% D^+ at 4.03 GeV[31] (which is appropriate to the DASP data). It is important to keep in mind that the detection efficiencies which have been used in these measurements have been derived on the assumption of equal D^0 and D^+ semi-leptonic branching ratios. If they are different, then the D branching ratio of 8.0% cannot be simply interpreted as the arithmetic mean, weighted by the D^0 and D^+ fractions.

The electron momentum spectrum of the multiprong events observed by DELCO[39] at the ψ" is shown in Fig. 28. This data is uncorrected for the Cerenkov

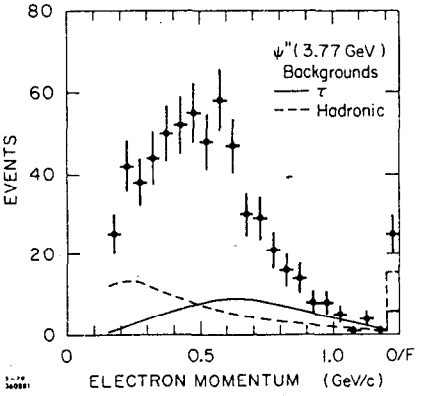

Fig. 28. The electron momentum spectrum from multiprong events observed by DELCO at the ψ". The solid curve indicates the predicted contribution from τ decays (19% of the observed events). The dashed curve shows all other sources of background (24%).

detection efficiency or the backgrounds due to the τ and hadronic events. The latter are determined from data taken at the ψ and at 3.50 - 3.52 GeV, and also by independent calculations. After correcting for these

effects, the D electron spectrum (Fig. 29) is obtained and compared with several hypotheses which assume the

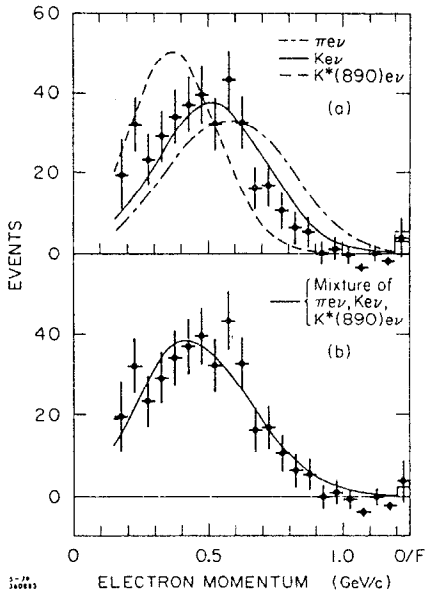

Fig. 29. The electron momentum spectrum from D decays at the ψ", measured by DELCO. The curves have been fitted to the data below 1 GeV/c and correspond to the following hypotheses:
a) $D \to \pi e\nu$ (dot-dashed curve, $\chi^2/dof = 80.9/16$), $D \to Ke\nu$ (solid curve, $\chi^2/dof = 23.4/16$), $D \to K^*(890)e\nu$ (dashed curve, $\chi^2/dof = 53.8/16$).
b) Contributions from $D \to Ke\nu$ (55%), $D \to K^*e\nu$ (39%) and $D \to \pi e\nu$ (6%) $\{\chi^2/dof = 11.2/15\}$.

GIM mechanism for the D semi-leptonic decays. The spectrum is incompatible with a single decay mode but shows good agreement with a mixture of $Ke\nu$ and $K\pi e\nu$. The fitted contributions depend on the fraction of the $K\pi$ mode which is resonant. The extreme values are (37 ± 16)% and (55 ± 14)% for $K^*e\nu$ and $Ke\nu$, respectively, or, in the case of non-resonant $K\pi$ production, (55 ± 21)% and (38 ± 19)% for $K\pi e\nu$ and $Ke\nu$, respectively. In these fits a small contribution from $\pi\pi e\nu$ and $\pi e\nu$ is included and fixed in relation to the Cabibbo-favored channel. A study was also made of the possible contribution of the channels $K\pi\pi e\nu$, $Q(1280)e\nu$ and $K^{**}(1420)e\nu$ and in all cases the fits were compatible with zero signal.

VII. The Charm Lifetime

The relative lifetime of the D^+ and D^0 can be investigated by measuring the individual D^+ and D^0 semi-leptonic branching ratios. This follows since the dominant decay, $c \to se^+\nu_e$, is $\Delta I = 0$ and so there exists a pairwise equality of each D^0 and D^+ semi-leptonic decay channel, e.g., $\Gamma(D^0 \to K^-e^+\nu_e) = \Gamma(D^+ \to \bar{K}^0e^+\nu_e)$ and $\Gamma(D^0 \to \bar{K}^0\pi^-e^+\nu_e) = \Gamma(D^+ \to K^-\pi^+e^+\nu_e)$. In consequence, the relative lifetimes $\tau(D^+)/\tau(D^0) = b(D^+ \to e\nu X)/b(D^0 \to e\nu X)$. This measurement can in turn be converted into an absolute lifetime determination since the decay rate $\Gamma(D \to Ke\nu)$ can be reliably calculated,[40] in analogy with $\Gamma(K \to \pi e\nu)$, with a small uncertainty arising from form-factor effects.

The experimental techniques which can separate the D^+ and D^0 semi-leptonic branching ratios are: a) measuring the multi-prong electron cross-section at two energies with known, and different, D^0 and D^+ compositions, b) utilizing a soft π^+ tag in $D^{*+}D^-$ events to signal the presence of a D^0 and a D^-, c) tagging events by hadronic decays at the ψ", and finally d) comparing the production rate of one-electron and two-electron events.

The last technique has been applied to the DELCO data sample (Table XII) at the ψ". As a check that the

Table XII. The DELCO Multi-Prong Electron Data Sample at the ψ"

Event Description	Event Topology: 1 electron	2 electrons	2 electrons + "V" (K^0_S)
Observed	1416	21	8
Background	692	4.6	1.8
Charm Signal	724	16.4	6.2

events are predominantly consistent with both D mesons decaying semi-leptonically, the electron energy spectra for the 1e (background-subtracted) and 2e (unsubtracted) data are compared in Fig. 30.

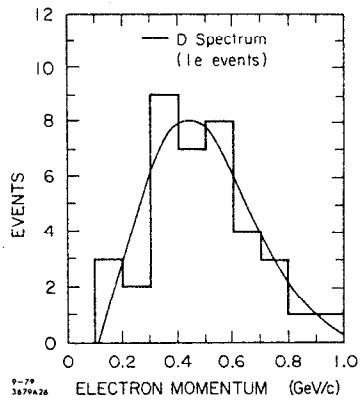

Fig. 30. The electron momentum spectrum of the multi-prong, 2-electron events (e^+e^- + ≥ 1-charged-particle) observed by DELCO at the ψ". The curve indicates the charm spectrum observed in the 1-electron events.

The observed number of 1e events from charm (N_1) is related to the D^0 and D^+ semi-leptonic branching ratios (b^0 and b^+, respectively) by the expression, $N_1 = A^0_1 2b(1-b^0) + A^+_1 2b^+(1-b^+)$, where the constant $A^0_1(A^+_1)$ is the number of $D^0D^0(D^+D^-)$ decays in the data-sample, multiplied by the detection efficiency. The equivalent expression for the 2e events is, $N_2 = A^0_2 b^{0\,2} + A^+_2 b^{+\,2}$, where A^0_2 and A^+_2 involve new detection efficiencies. Thus we see that there is a band of solutions for b^0 and b^+ which is approximately linear for the 1e data and elliptical for the 2e data. The results are shown in Fig. 31 for the two extreme assumptions in detection efficiency. The data indicates either $b^+ >> b^0$ or $b^+ << b^0$, independent of assumptions about the individual semi-leptonic decay channels. In order to assess the significance of this data, we can ask, "What is the probability of observing twenty-one 2e events or more, if $b^0 = b^+$?" For $b^0 = b^+ = 8\%$, the predicted number of 2e events (including background) is 10.5 and the probability of observing ≥ 21 is 0.3%. (This calculation assumes a K/K^* ratio which leads to the largest, and therefore most conservative, number of 2e events.) If we take $b^0 = b^+ = 9.1\%$, which is 1σ above the world average value, the predicted number is 12.2 and the probability, 1.3%. For comparison, if we predict 21, the probability of observing 21 or more is, of course, 50%. It is therefore unlikely that the excess 2e events are a statistical fluctuation.

In order to distinguish between the two overlap regions in Fig. 31 the K^0_S ("V") content in the 2e events is utilized. The presence of a K^0_S is signified by at least one track which does not project back towards the origin in the azimuthal view.

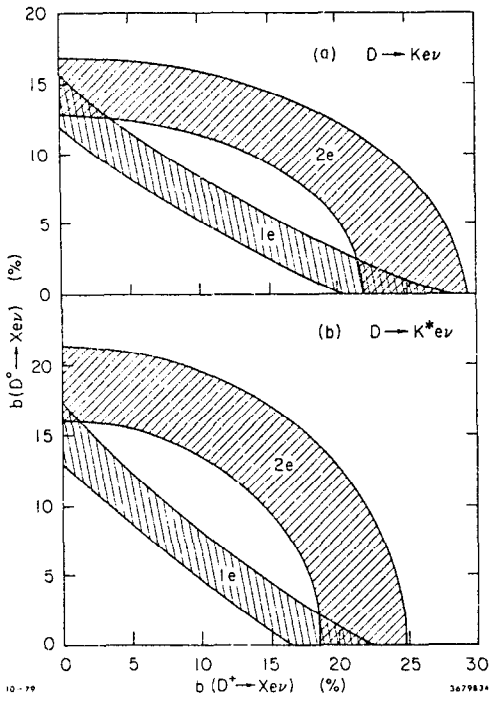

Fig. 31. The allowed solutions for the D^0 and D^+ semi-leptonic branching ratios in the DELCO 1e and 2e multiprong data at the ψ''. The shaded regions, which correspond to $\pm 1\sigma$ limits, are ploted for two extreme assumptions of the detection efficiencies: a) all $D \to Ke\nu$ and b) all $D \to K^*e\nu$.

The information which is summarized in Table XIII is the probability of observing eight 2eV events or more given 16.4 charm 2e events, for several D decay modes. Note that this information is independent of the absolute number of 2e events since it relies on the fraction with a "V".

Table XIII. The Probabilities of Observing Eight 2eV Events or More

Decay Mode	Predicted Number of 2eV Events†	Probability (%)
$D^+D^- \to K^0e\nu$	7.9	53
$K^{*0}e\nu$	3.2	1.7
$D^0\overline{D^0} \to K^\pm e\nu$	1.8	0.05
$K^{*\pm}e\nu$	3.5	2.8

†including 1.8 background events.

The large observed K^0_S signal in the 2e events therefore implies: a) there is a large contribution from D^+D^- and b) $D^+ \to \bar{K}^0e^+\nu_e$ is an important decay channel.

Finally, by combining the information from the 1e, 2e and 2eV/2e data (Fig. 32), the D^0 and D^+ semi-electronic branching ratios are found to be < 5% (95% CL) and (24 ± 4)%, respectively. These preliminary values account for systematic uncertainties such as the fractions of Kev and $K^*e\nu$. The Mark II data also favors a value for the D^+ semi-electronic branching ratio which is larger than that of the D^0. The preliminary measurements[32] are $b^0 = (5.2 \pm 3.3)$% and $b^+ = (16 \pm 5.3)$%, using tagged events at the ψ''. These

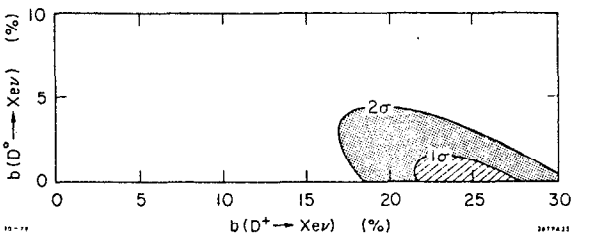

Fig. 32. The probability contour plot for the D^0 and D^+ semi-electronic branching ratios, measured by DELCO.

measurements are consistent with the observation (Fig. 27) that the inclusive electron yield from charm events is largest at the ψ'', where the D^+ fraction is a maximum.

The results imply that the D^+ lives several times longer than the D^0; in the DELCO data $\tau(D^+)/\tau(D^0) > 4$ (95% CL). The actual lifetimes may be determined from the calculation,[40] $\Gamma(D \to Ke\nu) = (1.4 \pm 0.3)\,10^{11}\ \text{sec}^{-1}$, and assuming a Kev/Xev fraction of (45 ± 24)% (which corresponds to the limits indicated by the 1e momentum distribution). The values for the DELCO data are: $\tau(D^0) < 3.5\ 10^{-13}$ sec (95% CL) and $\tau(D^+) = (8 \pm 5)\ 10^{-13}$ sec. A similar lifetime-difference has been indicated by direct observations in emulsions and bubble-chambers.[41] Based on a world total of about a dozen events in each class, the mean lifetime of the neutral charmed particles is $1.0\ 10^{-13}$ sec, compared with $5.3\ 10^{-13}$ sec for the charged charmed particles.

The observed inequality of the D^0 and D^+ lifetimes implies that the simple view of nonleptonic decays, in which the spectator quark plays an unimportant role, is incorrect. This picture implies $\Gamma^0_{NL} = \Gamma^+_{NL}$, whereas the DELCO measurements indicate $\Gamma^0_{NL} > 5.3\ \Gamma^+_{NL}$ (95% CL). Several authors[42] had previously advocated this possibility based on their considerations of the D and D^+ branching ratios, particularly involving $K\pi$ final states.

VIII. Conclusion

The studies of the τ and charmed particles are by no means complete and for the future we will continue to rely largely on e^+e^- data at these energies. Amongst the topics of particular interest are:

1) How exact is e-μ-τ universality? This is explored by improved measurements of the τ lifetime, V - A current, ν_τ mass and rare decay modes.

2) The Cabibbo angle in τ decays. The most readily accessible measurement is $K^{*-}\nu_\tau/\rho^-\nu_\tau$.

3) The characteristics of the τ multiprong decays, particularly the "A_1"ν mode.

4) The values of R (within a 2% error) above and below charm threshold.

5) The charmonium states η_c, η_c' and $^1P_1$.

6) Confirmation of the DASP observation of the F mesons and measurement of their properties.

7) Identification of further charmed baryon states and measurement of the branching ratios, particularly of the semi-leptonic decays since these may be an important source of prompt leptons in other interactions.

8) Measurement of the Cabibbo angle in charm decays from the relative rates, $\Gamma(D^+ \to \pi^0e^+\nu_e)/\Gamma(D^+ \to K^0e^+\nu_e)$.

Although there is still plenty of work to be done, it is becoming experimentally increasingly difficult. For example, D measurements will require almost a full

years run in order to decrease the typical statistical errors by a factor of two. With luck this picture may be tempered by new productive E_{cm} regions and the possibilities of improved luminosities. If this last year is to be a guide, we can expect some more surprises—even from the D mesons with which we are most familiar.

It is a pleasure to thank Charles Brown and John Peoples for their hospitality at the Fermilab Conference. In addition, I wish to thank the experimentalists at DORIS and SPEAR for discussions of their unpublished data. Finally, I warmly thank my colleagues in the DELCO collaboration for their most enjoyable and informative company.

References

1. R. Bradelik et al. (DASP), Phys. Lett. 73B, 109 (1978); W. Bacino et al. (DELCO), Phys. Rev. Lett. 41, 13 (1978); W. Bartel et al. (DESY-HEIDELBERG), Phys. Lett. 77B, 331 (1978).
2. Y. S. Tsai, SLAC preprint SLAC-PUB-2105 (1978).
3. G. L. Kane and S. Raby have indicated (UMHE 79-26 and in the discussion period following this talk) that the present experimental tests cannot completely exclude a spin 3/2 assignment for the τ. It is certainly possible to reduce the divergent high energy cross section expected under this spin assignment by the introduction of a form factor. However, the calculations of $\Gamma(\tau^- \to \pi^- \nu_\tau) / \Gamma(\tau^- \to e^- \bar{\nu}_e \nu_\tau)$ have been made by the authors of Reference 9 under completely general assumptions of the couplings, and a comparison with the experimental measurements excludes a spin 3/2 assignment for either τ or ν_τ. I wish to thank F. J. Gilman for discussions on this point.
4. W. Bacino et al., Phys. Rev. Lett. 42, 749 (1979),
5. O. Nachtmann and A. Pais, Phys. Rev. D16, 630 (1977).
6. G. J. Feldman, invited talk at the International Meeting on the Frontier of Physics, Singapore, SLAC preprint SLAC-PUB-2230 (1978),
7. F. J. Gilman and D. H. Miller, Phys. Rev. D17, 1846 (1978), N. Kawamoto and A. I. Sanda, DESY 78/14 (1978).
8. The details of the Mark II data are discussed by V. Lüth at this conference.
9. Y. S. Tsai, Phys. Rev. D4, 2821 (1971), M. B. Thacker and J. J. Sakurai, Phys. Lett. 36B, 103 (1971), C. P. Korthals-Altes and P. Mery, Phys. Lett. 72B, 375 (1978), Y. Ahn, J. Kim and M. S. Song, Phys. Lett. 73B, 196 (1978), W. Alles, Bologna 79-0441 (1979).
10. G. Flügge, private communication of an unpublished preprint. The earlier analysis, based on a somewhat smaller data sample, is reported by G. Alexander et al., Phys. Lett. 73B, 99 (1978).
11. J. J. Sakurai, p. 353, "Proceedings of the VII International Symposium on Lepton and Photon Interactions at High Energies," ed. W. T. Kirk, Stanford (1975).
12. A. M. Cnops et al., Phys. Rev. Lett. 40, 144 (1978).
13. G. Atarelli, XIX International Conference on High Energy Physics, Tokyo (1978) and Rome preprint 107 (1978).
14. F. J. Gilman, Kyoto Summer Institute for Particle Physics, Kyoto, Japan, SLAC preprint SLAC-PUB-2226 (1978).
15. M. Dine and J. Sapirstein, Phys. Rev. Lett. 43, 668 (1979), K. Chetyrkin, A. Kateev and F. Tkachov, Phys. Lett. 85B, 277 (1979).
16. R. M. Barnett, M. Dine and L. McLerran, SLAC preprint (in preparation). The Mark II data points are from Reference 19a.
17. J. D. Bjorken, SLAC preprint SLAC-PUB-2366 (1979).
18. E. Eichten, K. Gottfried, T. Kinoshita, K. Lane and T. Yan, Phys. Rev. D17, 3090 (1978) and CLNS-425, submitted to Phys. Rev. D (1979).
19. The data of Fig. 14 is due to a) J. Siegrist, Ph.D. thesis (unpublished), b) J. Burmester et al., Phys. Lett. 66B, 395 (1977), c) A. Petersen, Ph.D. thesis, DESY F22-78/06 (1978), d) W. Bacino, Ph.D. thesis (unpublished), e) E. Bloom, invited talk at this conference.
20. E. Bloom, invited talk at this conference.
21. E. Bloom, invited talk at the XIV Recontre de Moriond, Les Arcs-Savoie, France (1979).
22. R. Brandelik et al., Z. Physik C, Particles and Fields 1, 233 (1979).
23. P. Jenni, private communication, and V. Lüth, invited talk at this conference.
24. E. G. Cazzoli et al., Phys. Rev. Lett. 34, 1125 (1975).
25. B. Knapp et al., Phys. Rev. Lett. 37, 882 (1976).
26. P. Schreiner, invited talk at this conference.
27. A. Kernan, invited talk at this conference.
28. G. S. Abrams et al., submitted to Phys. Rev. Lett. and SLAC preprint SLAC-PUB-2406 (1979).
29. This measurement of $R(\Lambda + \bar{\Lambda})$ is approximately a factor of 2 larger than the value previously reported by M. Picolo et al., Phys. Rev. Lett. 39, 1503 (1977). Most of the discrepancy originates in the failure to account for losses of the soft pions from Λ decays in the earlier analysis.
30. G. J. Geldman, Banff Summer Institute on Particles and Fields, SLAC preprint SLAC-PUB-2068 (1977).
31. P. A. Rapidis, Ph.D. thesis, SLAC-220 (1979).
32. R. Schindler, Ph.D thesis, SLAC-219 (1979), and V. Lüth, invited talk at this conference.
33. V. Vuillemin et al., Phys. Rev. Lett. 41, 1149 (1978).
34. J. M. Feller et al., Phys. Rev. Lett. 41, 274 (1978).
35. G. S. Abrams et al., submitted to Phys. Rev. Lett. and SLAC preprint SLAC-PUB-2337 (1979).
36. A "naïve" theory is, by definition, one which fails to agree with experiment. (In fairness, there are also "naïve" experiments!).
37. H. Harari, invited talk at this conference.
38. B. H. Wiik and G. Wolf, DESY-78/23 (1978).
39. W. Bacino et al., Phys. Rev. Lett. 43, 1073 (1979).
40. See, for example, D. Fabirov and B. Stech, Nucl. Phys. B133, 315 (1978). Further references are found in Ref. 39.
41. L. Voyvodic, invited talk at this conference.
42. M. Katuya, Phys. Rev. D18, 3510 (1978). Y. Hara, submitted to Progr. Theor. Phys. (1979); M. Katuya and Y. Koide, Phys. Rev. D19, 2631 (1979).